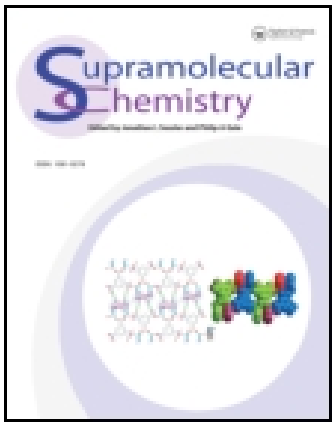

Supramolecular Chemistry
Publication details, including instructions for authors and subscription information:
http://www.tandfonline.com/loi/gsch20

Spectroscopic and computational studies on the development of simple colorimetric and fluorescent sensors for bioactive anions

Darshna Sharma [a] , Ankit R. Mistry [a] , Rati Kanta Bera [b] & Suban K. Sahoo [a]

[a] Department of Applied Chemistry , SV National Institute of Technology (SVNIT) , Surat , 395007 , Gujrat , India

[b] Department of Chemistry , Sant Longowal Institute of Engineering and Technology , Longowal , 148106 , Punjab , India

Published online: 19 Dec 2012.

To cite this article: Darshna Sharma , Ankit R. Mistry , Rati Kanta Bera & Suban K. Sahoo (2013) Spectroscopic and computational studies on the development of simple colorimetric and fluorescent sensors for bioactive anions, Supramolecular Chemistry, 25:4, 212-220, DOI: 10.1080/10610278.2012.752092

To link to this article: http://dx.doi.org/10.1080/10610278.2012.752092

Supramolecular Chemistry, 2013
Vol. 25, No. 4, 212–220, http://dx.doi.org/10.1080/10610278.2012.752092

Spectroscopic and computational studies on the development of simple colorimetric and fluorescent sensors for bioactive anions

Darshna Sharma[a], Ankit R. Mistry[a], Rati Kanta Bera[b] and Suban K. Sahoo[a]*

[a]*Department of Applied Chemistry, SV National Institute of Technology (SVNIT), Surat 395007, Gujrat, India;* [b]*Department of Chemistry, Sant Longowal Institute of Engineering and Technology, Longowal 148106, Punjab, India*

(*Received 6 July 2012; final version received 19 November 2012*)

Spectroscopic techniques (UV–vis and fluorescence) and computational (HF/6-31G(d,p)) methods were adopted to investigate the anion recognition ability of two novel Schiff base receptors ($\mathbf{L^1}$ and $\mathbf{L^2}$) synthesised from the condensation of 5-nitrosalicylaldehyde and 2-aminophenol or 2-aminothiophenol. Both the receptors portrayed a visually detectable colour change upon addition of fluoride, acetate and dihydrogen phosphate anions from light yellow ($\mathbf{L^1}$) or colourless ($\mathbf{L^2}$) to yellow due to the formation of hydrogen bonding complexes in 1:1 stoichiometry and/or deprotonation between these anions and the receptors. No significant colour change was observed upon addition of other anions such as chloride, bromide, iodide and hydrogen sulphate.

Keywords: anion recognition; colorimetric and fluorescent sensors; Schiff bases; HF/6-31G(d,p)

1. Introduction

There is bourgeoning interest in the design and synthesis of suitable receptor for the selective encapsulation and sensing anions such as acetate, fluoride and dihydrogen phosphate (DHP) due to their important roles in biomedicinal, environmental and chemical processes (*1–5*). Among the various types of sensing techniques, the development of anion-selective sensors through the naked eye (colorimetric) and fluorescent responses has attracted considerable attention because of their ability to provide a simple, sensitive, selective, precise and economical method for online monitoring up to very low concentrations of target anions. In designing such anion sensors, the receptor unit should have the potential to bind or interact with the target anion (analyte) selectively and efficiently through either electrostatically or hydrogen bonding, and also the binding unit must be connected suitably to a light-emitting group (fluorophore unit) that produces a distinct signal during the anion recognition procession (*6–8*). With regard to the binding sites, the functional groups such as amine, urea, thiourea, amide, imidazolium, pyrroles and phenolic-OH are numerously used owing to their ability to perform as hydrogen donors (*9–15*).

Among the various bioactive anionic analytes, acetate is one of the biochemically important anions because it acts as a critical component in numerous metabolic processes (*16*). Also, the rate of acetate production and oxidation has been frequently used as an indicator of organic decomposition in marine sediments (*17*). Therefore, the design of acetate-selective receptor is particularly challenging for investigators. Many examples are available about the acetate-selective sensor molecules in the literature (*9–15*), but most of the sensors have complicated structures that are synthesised by multi-step procedures and also interfered due to the presence of competitive anions. As an alternative, Schiff bases are widely investigated in the recent times for detecting anions by both colorimetric and fluorimetric methods because of their simple one-step synthetic procedure (*18–28*). Herein, we have investigated the anion recognition ability of two novel Schiff bases (Figure 1) 2-((2-hydroxyphenylimino)methyl)-4-nitrophenol ($\mathbf{L^1}$) and 2-((2-mercaptophenylimino)methyl)-4-nitrophenol ($\mathbf{L^2}$) by experimental (UV–vis and fluorescence) and computational (HF/6-31G(d,p)) methods.

2. Results and discussion

2.1 Design of anion sensors

The anion recognition behaviour of the receptor $\mathbf{L^1}$ containing two phenolic-OH as anion-binding units was investigated recently towards anions such as F^-, Cl^-, Br^- and OH^- (*29*). It was reported that the receptor $\mathbf{L^1}$ showed colorimetric and 'turn-off' fluorescent responses in the presence of high electronegative and small-size anions F^- and OH^- because of their ability to form intermolecular hydrogen bonding and/or deprotonating phenolic-OH proton. The ^{1}H NMR spectral data supported the anion recognition with the disappearance of the OH proton peak attached to the nitro-substituted aromatic ring and the shifting of other OH and imine (CH═N) proton peaks.

*Corresponding author. Email: suban_sahoo@rediffmail.com

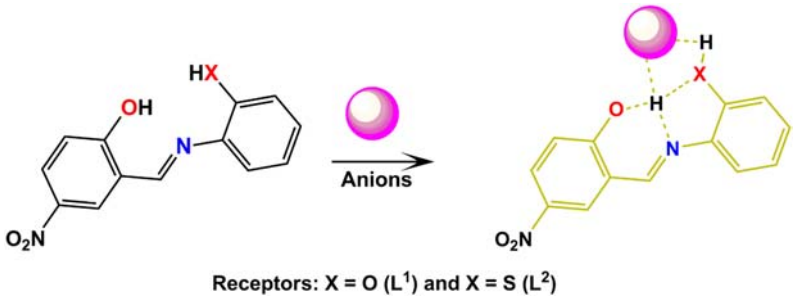

Figure 1. Designing of anion sensors based on receptors $\mathbf{L^1}$ and $\mathbf{L^2}$.

However, as the sensing ability of an artificial neutral receptor towards anions depends on factors such as conformational complementarity and anion basicity, we thought the triangular (Y-shaped) shaped acetate anion might be fittest to make multiple hydrogen bonds with the receptor $\mathbf{L^1}$ with higher selectivity and efficiency among the various bioactive anions including fluoride. This assumption was well supported by the results reported recently with a positional isomer of $\mathbf{L^1}$, which showed acetate-selective colorimetric response in aqueous acetonitrile (*30*). Therefore, we wish to examine again the anion sensing ability of $\mathbf{L^1}$ towards anions such as AcO^-, $H_2PO_4^-$, HSO_4^-, F^-, Cl^-, Br^- and I^-. Also, for comparison, we have investigated a new receptor $\mathbf{L^2}$ containing one phenolic-OH and another thiophenol-SH as anion recognition units.

Firstly, the colorimetric response of the Schiff base receptors $\mathbf{L^1}$ and $\mathbf{L^2}$ (5.0×10^{-5} M) in acetonitrile has been investigated before and after the addition of equivalent amount of each anion to evaluate the anion recognition properties. As shown in Figures 2(a) and 3(a), we observed a detectable colour change from light yellow ($\mathbf{L^1}$) or colourless ($\mathbf{L^2}$) to yellow in the presence of AcO^-, F^- and $H_2PO_4^-$ anions. However, no obvious colour change was observed in the presence of HSO_4^-, Cl^-, Br^- and I^- in both the receptors, even the anions were excessive presumably due to weaker interactions with the receptors that failed to alter any structural changes. In addition, it was observed that the intensity of colour decreases reversibly on addition of small amount of water (Figure S1 of the Supplementary Information, available online). The presence of protic solvents such as water can compete with anions for binding sites and disturb the H-bond interactions between the host and the anionic guest that lead to a reversal of the visual colour (*21*).

Secondly, the UV–vis experiments of the receptors $\mathbf{L^1}$ and $\mathbf{L^2}$ in acetonitrile were carried out in the absence and presence of anions such as AcO^-, $H_2PO_4^-$, HSO_4^-, F^-, Cl^-, Br^- and I^- (Figures 2(b) and 3(b)). Receptor $\mathbf{L^1}$ exhibited a light yellow colour in solution because of the absorption band with maxima at ~440 nm due to $n \rightarrow \pi^*$ transition. The appearance of peak above 400 nm indicates the presence of ketoenamine form of $\mathbf{L^1}$ in solution because of the electron-withdrawing NO_2 group that enhances the acidity of the phenolic-OH group to favour the tautomeric transformation from enolimine to ketoenamine form. In contrast to $\mathbf{L^1}$, $\mathbf{L^2}$ exhibited a colourless solution due to a weak absorption at ~430 nm that also indicate predominantly the enolimine form of $\mathbf{L^2}$ in solution. On addition of equivalent amount of various anions, obvious hyperchromic spectral shift at 440 nm for $\mathbf{L^1}$ and 430 nm for $\mathbf{L^2}$ was observed in the order $AcO^- > F^- > H_2PO_4^-$ and $AcO^- \approx F^- > H_2PO_4^-$, respectively. The variations in the absorbance bands are due to the recognition of the receptors with the hydrogen bond-forming anions, which reduce the O—H bond strength and facilitate deprotonation to increase charge delocalisation. Alternatively, addition of anionic species favoured the formation of ketoenamine form that intensified the yellow

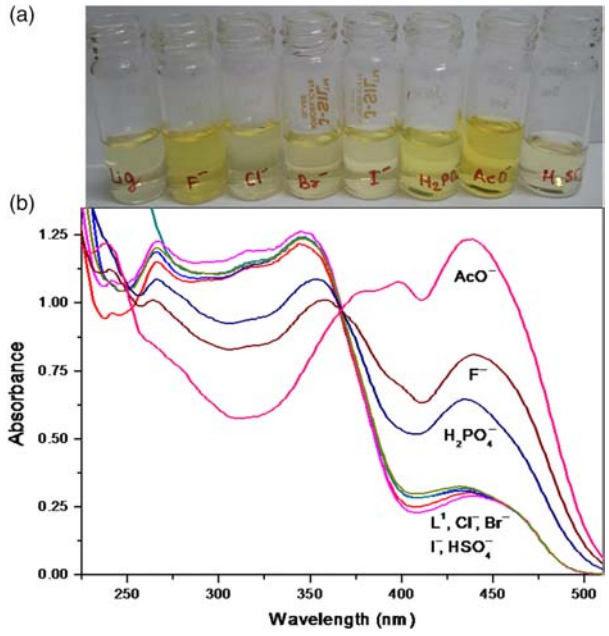

Figure 2. Colour changes (a) and UV–vis spectra (b) of the receptor $\mathbf{L^1}$ (5.0×10^{-5} M, vial was mentioned as **Lig**) in the absence and presence of 1 equivalent of different anions (Colour Online).

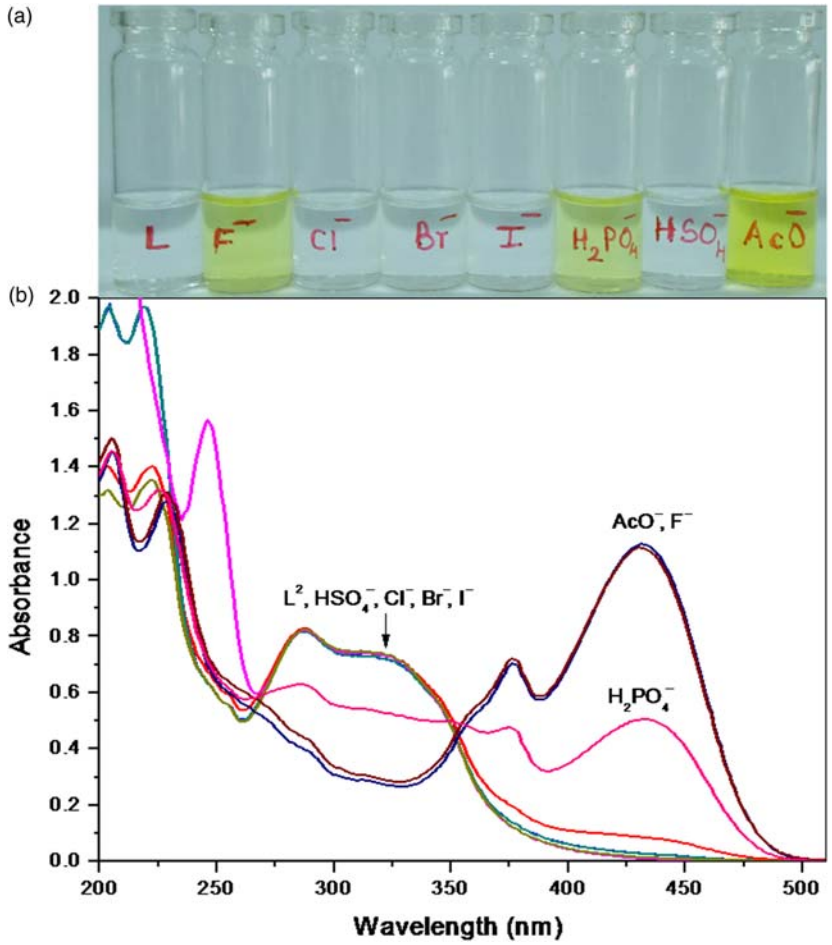

Figure 3. Colour changes (a) and UV–vis spectra (b) of the receptor $\mathbf{L^2}$ (5.0×10^{-5} M, vial was mentioned as **L**) in the absence and presence of one equivalent of different anions (Colour Online).

colouration. However, the appearance of new peak at 375 nm on addition of anions indicates the participation of O—H groups of the receptors $\mathbf{L^1}$ and $\mathbf{L^2}$ in anion recognition process. In contrast, upon addition of other anions, no noticeable spectral changes were observed.

In order to elucidate the possible structure of the receptors $\mathbf{L^1}$ and $\mathbf{L^2}$, the geometries of the receptors and their tautomeric forms were optimised using the HF/6-31G(d,p) method in both gas phase and acetonitrile. From the optimised structure of receptors $\mathbf{L^1}$ and $\mathbf{L^2}$ (Figure 4), it can be observed that the two possible binding sites (i.e. phenolic-OH/thiophenol-SH groups) are present in the same side, and therefore no apparent conformational changes in the receptors are required for the encapsulation of the incoming anions. The calculated results on relative energy and the energy gap of E_{LUMO}, E_{HOMO} of the receptors $\mathbf{L^1}$ and $\mathbf{L^2}$ and their tautomers are listed in Table 1. From Table 1, it can be observed that the relative energy between the enolimine and ketoenamine forms for $\mathbf{L^2}$ is higher than that of $\mathbf{L^1}$ in both gas phase and acetonitrile medium. In case of $\mathbf{L^1}$, the relative energy in gas phase (22.88 kJ mol^{-1}) decreases to 3.73 kJ mol^{-1} in acetonitrile, which indicates that the tautomeric equilibrium (enolimine ↔ ketoenamine) was moved from left towards the right in acetonitrile and therefore both ketoenamine and enolimine forms could be present. However, the relative energy for $\mathbf{L^2}$ in both gas phase (33.42 kJ mol^{-1}) and acetonitrile (15.44 kJ mol^{-1}) is higher for tautomeric transformation. Furthermore, the calculated band gap ΔE ($\Delta E = E_{LUMO} - E_{HOMO}$) of enolimine form is larger than that of its ketoenamine tautomer. Thus, the ketoenamine form of the receptors with lower band gap may be responsible for the light yellow colouration and absorbance at longer wavelength.

2.2 *UV–vis titrations*

The spectrophotometric titrations of the receptors $\mathbf{L^1}$ and $\mathbf{L^2}$ with the anions (AcO^-, F^- and $H_2PO_4^-$) have been performed in acetonitrile to calculate the binding constant (K) for the respective anions. Upon successive addition of anions to a fixed concentration of the receptors, $\mathbf{L^1}$ and $\mathbf{L^2}$

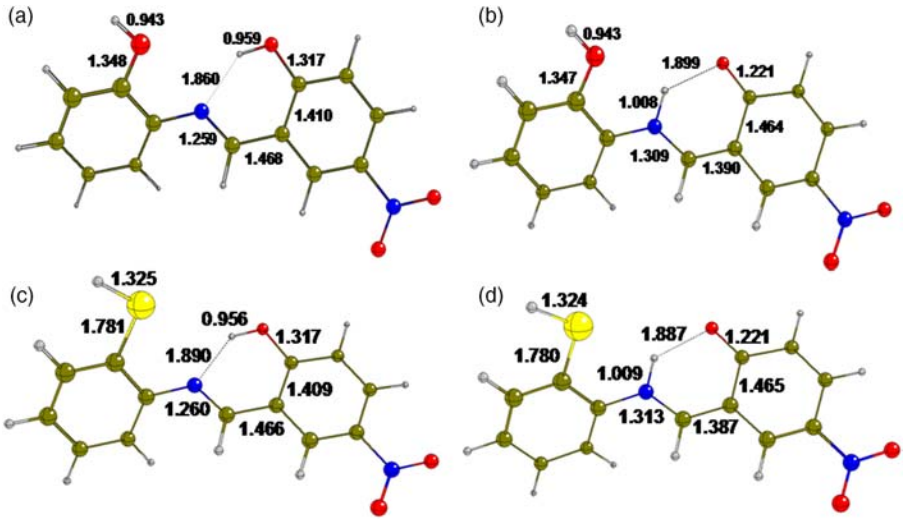

Figure 4. Optimised structure of $\mathbf{L^1}$ (a) and $\mathbf{L^2}$ (c) and their ketoenamine form (b and d) with selected bond lengths (Å) in gas phase by HF/6-31G(d,p) method.

resulted in hyperchromic shift above 400 nm with the formation of isosbectic points, which indicate the formation of single complex species between the receptors and the anions added (Figure 5 and Figure S2 of the Supplementary Information, available online). The spectral data were used to calculate the binding constant (K) between the receptors and the anions by applying the Benesi–Hildebrand equation (*31*):

$$\frac{1}{A - A_0} = \frac{1}{A_{max} - A_0}\left[\frac{1}{K[X_0]} + 1\right], \qquad (1)$$

where A is the absorbance measured with different concentrations of the anions, A_0 is the absorbance of the free receptor, A_{max} is the maximum absorbance of receptor and anions, X_0 is the concentration of the anions added and K is the association constant. Then, the graphs were plotted between $1/(A - A_0)$ against $1/[X_0]$, and the binding constant (K) was determined from the ratio of intercept/slope. The calculated binding constants (K) for the receptors $\mathbf{L^1}$ and $\mathbf{L^2}$ towards AcO^-, F^- and $H_2PO_4^-$ anions are summarised in Table 2.

Obviously from Figures 2(b), 3(b) and Table 2, the trends for the anion-binding abilities were determined to be $AcO^- > F^- > H_2PO_4^-$ for $\mathbf{L^1}$ and $AcO^- \approx F^- > H_2PO_4^-$ for $\mathbf{L^2}$. The trend can be explained with the following principles: (i) the ability to hold the multiple hydrogen-bonding interactions between the hosts and the anionic guests, (ii) the shape complementarity between the receptor and the anions and (iii) alkalescence of interacting anions and nature of the binding sites of receptor. The higher acetate recognition ability of receptor $\mathbf{L^1}$ was presumably due to the shape complementarity of $\mathbf{L^1}$ with the two phenolic-OH binding sites forming multiple hydrogen bonds with acetate anions. Also, the alkalescence of acetate anion was higher than the other anions. In contrast to $\mathbf{L^1}$, $\mathbf{L^2}$ with both OH and SH binding sites showed similar affinity towards fluoride and acetate. However, both the receptors showed lower binding ability for the tetrahedrally shaped $H_2PO_4^-$.

The selectivity of the host for a specific anion of interest could be rationalised on the basis of not only by the by guest basicity but also by the complementary shape and stoichiometry between the host and the anion guest. Hence, the stoichiometry analysis of the receptors $\mathbf{L^1}$ and $\mathbf{L^2}$ with the anions was done using Job's plot method. The Job's plots (Figure S3 of the Supplementary Information,

Table 1. Calculated relative energy [$E_{relative} = E_T$(ketoenamine)$-E_T$(enolimine)] and energy gap ΔE ($\Delta E = E_{LUMO}-E_{HOMO}$) of $\mathbf{L^1}$, $\mathbf{L^2}$ and their tautomer obtained at HF/6-31G(d,p).

Parameters	Gas (acetonitrile)			
	$\mathbf{L^1}$	Tautomer of $\mathbf{L^1}$	$\mathbf{L^2}$	Tautomer of $\mathbf{L^2}$
$E_{relative}$ (kJ mol^{-1})	0 (0)	22.88 (3.73)	0 (0)	33.42 (15.44)
E_{LUMO} (a.u.)	0.06327 (0.05998)	0.04463 (0.04859)	0.05684 (0.05812)	0.04307 (0.04843)
E_{HOMO} (a.u.)	−0.30888 (−0.30439)	−0.29476 (−0.29749)	−0.30967 (−0.30568)	−0.30195 (−0.30282)
ΔE (kJ mol^{-1})	977.08 (956.65)	891.07 (908.63)	962.27 (955.15)	905.85 (922.21)

Note: 1 Ha = 2625.5 kJ mol^{-1}.

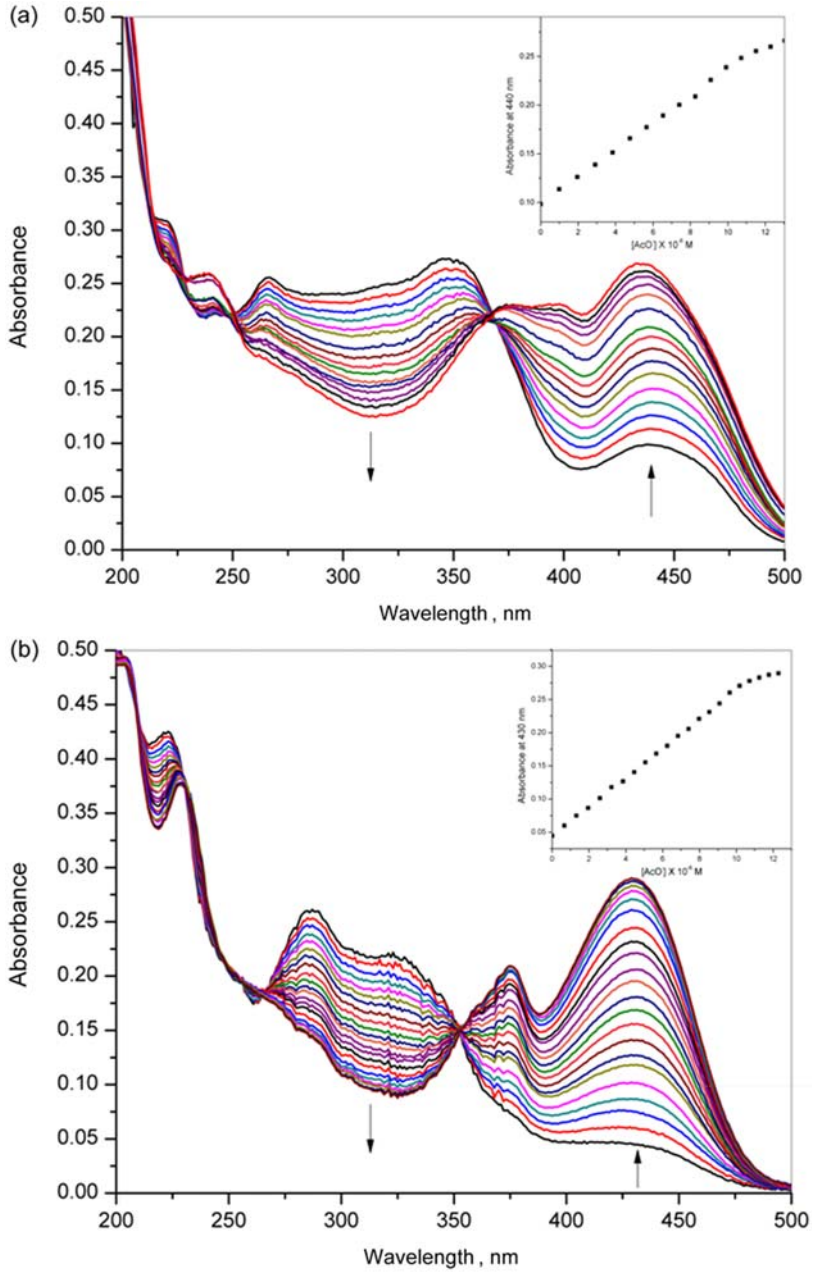

Figure 5. UV–vis spectra of the receptors (1.0×10^{-5} M) $\mathbf{L^1}$ (a) and $\mathbf{L^2}$ (b) with different equivalents of AcO^-. Inset shows the absorbance at (a) 440 nm and (b) 430 nm as a function of AcO^- concentrations.

available online) for the receptors with AcO^-, F^- and $H_2PO_4^-$ inferred that all the anions bind with the receptor in the ratio 1:1. Furthermore, the variation in the absorption spectra (Figure 5) and the ^{1}H NMR spectrum (Figure S4 of the Supplementary Information, available online) obtained for the acetate–$\mathbf{L^1}$ complex indicates similar modes of complexation as reported for fluoride ion with $\mathbf{L^1}$ (*29*). The two phenolic-OH groups of $\mathbf{L^1}$ interact with acetate anions to form the 1:1 acetate–$\mathbf{L^1}$ complex. In addition, the imine proton peak of free $\mathbf{L^1}$ at 9.3 ppm was downfield shifted to 9.2 ppm, and the variations in the peaks of both the

Table 2. Binding constants (K) of the receptors $\mathbf{L^1}$ and $\mathbf{L^2}$ with the corresponding anions.

Anions	$\mathbf{L^1}$ (M^{-1})	$\mathbf{L^2}$ (M^{-1})
Acetate	2.85×10^3	2.62×10^4
Fluoride	2.22×10^3	2.12×10^4
DHP	1.35×10^3	1.58×10^3
Other anions	ND	ND

Note: ND, binding constant could not be determined.

aromatic ring protons indicate possible conformational changes in $\mathbf{L^1}$ during the encapsulation of acetate anion. Further to confirm the binding modes between the receptors and the anions, we performed the absorption titrations of $\mathbf{L^1}$ and $\mathbf{L^2}$ with tetrabutylammonium hydroxide (TBAOH), under identical conditions to those described for other anions. The results from these anion titrations are shown in Figure 6 and Figure S5 of the Supplementary Information, available online. The similar spectral and colorimetric changes observed for both AcO^- and OH^- indicate the formation of the same species in solution. Also, the results clearly demonstrate that both anions are functioning here as a base, giving rise to the deprotonation upon interaction with the receptors $\mathbf{L^1}$ and $\mathbf{L^2}$.

In order to predict the possible structure of the anion–receptor complex, structural optimisation was performed at HF/6-31G(d,p) level by focusing on the proposed binding modes between the receptors ($\mathbf{L^1}$ and $\mathbf{L^2}$) and the anions. The optimised global minimum structure of anion–receptor complexes clearly indicates that the

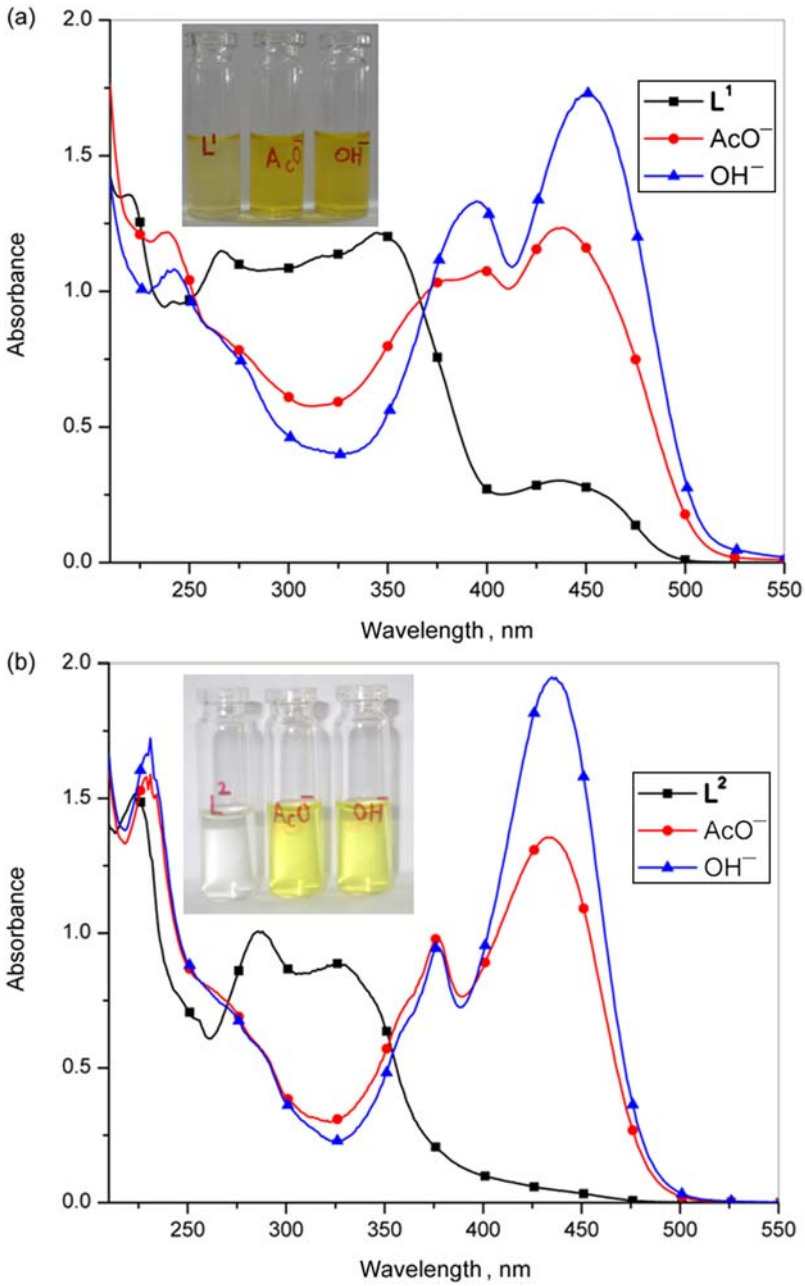

Figure 6. UV–vis spectra of the receptors (5.0×10^{-5} M) (a) $\mathbf{L^1}$ and (b) $\mathbf{L^2}$ in the absence and presence of equivalent amounts of AcO^- and OH^-. Inset shows the colour changes of the receptors upon addition of anions (Colour online).

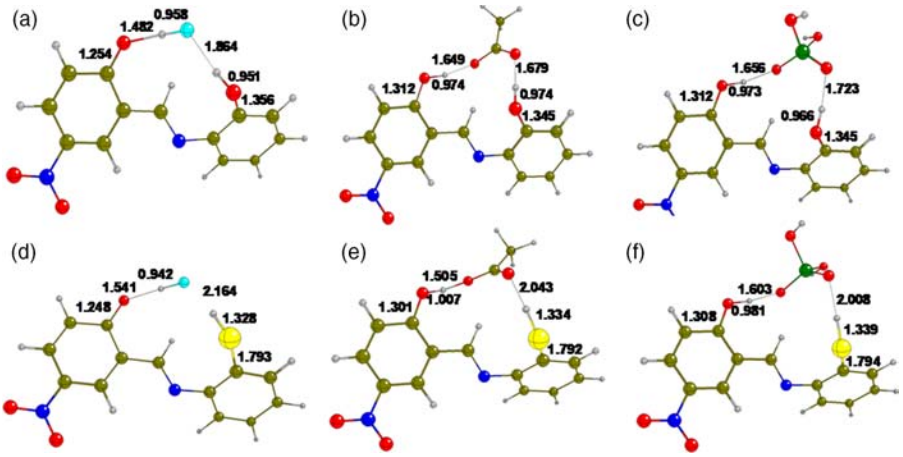

Figure 7. Optimised structure with selected bond lengths (Å) of anion–receptor complexes ($\mathbf{L}^1$: a–c and $\mathbf{L}^2$: d–f) in gas phase at HF/6-31G(d,p) method.

binding modes of receptors with fluoride, acetate and phosphate anions are almost similar. The phenolic-OH and thiophenol-SH moieties and the imine (CH═N) proton of the receptors interact with the anions to form a 1:1 anion–receptor complex. However, the optimised parameters shown in Figure 7 inferred that AcO^- is forming two similar and stronger hydrogen bonds than DHP. This is mainly due to the Y-shaped structure of the acetate anion that facilitates the formation of multiple hydrogen-bonded complex with the receptors than the tetrahedral-shaped DHP. However, due to higher electronegativity and small size, fluoride binds strongly only with OH group of 5-nitrosalicyladehyde but weakly with another OH/SH group. The lack of conformational complementary shape of fluoride anion to interact with $\mathbf{L}^1$ and $\mathbf{L}^2$ resulted weaker binding than acetate. Thus, proper orientation of the receptor for acetate anion recognition through hydrogen bonding and predicted stoichiometry obtained from the theoretical structural optimisation corroborates well with the experimental results.

2.3 *Fluorescence titrations*

The anion-binding behaviour of the sensor $\mathbf{L}^1$ was also investigated by fluorescence titrations in acetonitrile. The sensor $\mathbf{L}^1$ showed a strong emission band centred at 505 nm ($\lambda_{ex} = 450$ m) presumably due to the excited-state intramolecular proton transfer (ESIPT) process. The ESIPT is a well-known process in intramolecularly hydrogen-bonded Schiff bases, where a fast tautomeric transformation from enolimine to ketoenamine occurs in the excited states (*32*). Upon addition of acetate, there was a significant decrease in the emission intensity of $\mathbf{L}^1$ (Figure 8). Only 1 equivalent of acetate is sufficient to quench the emission intensity of $\mathbf{L}^1$. Addition of excess amount of acetate resulted no change in the emission spectrum of $\mathbf{L}^1$ (Figure S6 of the Supplementary Information, available online). The fluorescence quenching is occurred due to the blocking of ESIPT process on interaction of OH groups of $\mathbf{L}^1$ with acetate ion through hydrogen bonding followed by the intermolecular charge transfer. However, under similar condition, fluoride ions need 2 equivalents to quench the emission intensity of $\mathbf{L}^1$. Importantly, the quenching of $\mathbf{L}^1$ by acetate anion was not affected in the presence of other competitive anions. In contrast to $\mathbf{L}^1$, receptor $\mathbf{L}^2$ showed emission at 360 nm when excited at 275 nm. The emission of $\mathbf{L}^2$ was not affected noticeably on addition of acetate and fluoride anions (Figure S7 of the Supplementary Information, available online).

3. Conclusions

Two simple anion-selective chemosensors $\mathbf{L}^1$ and $\mathbf{L}^2$ were reported. Colorimetric and spectral titrations in acetonitrile inferred that (i) both the sensors showed visually detectable colorimetric responses on recognition with acetate, fluoride and DHP anions in 1:1 stoichiometry from light yellow (or colourless) to intense yellow, (ii) the detection limit ($3\sigma/S$) approximated from the spectral titrations for acetate anions with $\mathbf{L}^1$ and $\mathbf{L}^2$ is down to 4.57×10^{-7} and 1.72×10^{-7} M, respectively, (iii) the titrations with TBAOH demonstrate that the deprotonation event has a significant effect on the anion recognition process, (iv) the effect of anion was diminished by adding protic solvent and (v) the fluorescence of $\mathbf{L}^1$ was quenched whereas the fluorescence of $\mathbf{L}^2$ remains unchanged in the presence of AcO^- and F^-.

4. Experimental

4.1 *Materials and methods*

All the starting reagents and solvents used for the experiments were purchased commercially in the purest form and were used without further purification. All the

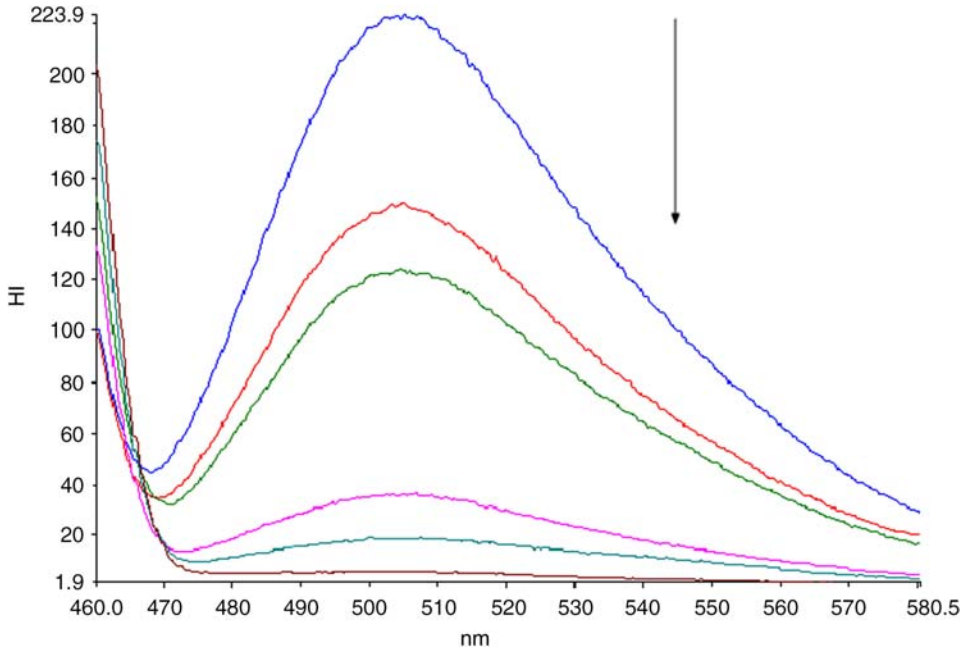

Figure 8. Changes in the emission spectrum of $\mathbf{L^1}$ (1.0×10^{-5} M) upon addition of AcO^- from 0 to 1.0×10^{-5} M in acetonitrile.

anions were used in the form of tetrabutyl ammonium salts [(n-$C_4H_9)_4NF$, (n-$C_4H_9)_4NCl$, (n-$C_4H_9)_4NBr$, (n-$C_4H_9)_4NI$, (n-$C_4H_9)_4NHSO_4$ and (n-$C_4H_9)_4NH_2PO_4$] and were purchased from Spectrochem Pvt. Ltd, Mumbai, India. The synthesis of the receptor $\mathbf{L^1}$ was done by following the available literature (*29*).

The absorption and fluorescence spectra were recorded in acetonitrile on a Cary 50 Varian UV–vis and PerkinElmer LS55 luminescence spectrophotometer, respectively, at room temperature by adopting a similar procedure. Stock solutions of the receptors (1.0×10^{-3} M) and anions (1.0×10^{-3} M) were prepared in acetonitrile. These solutions were used for all spectroscopic studies after appropriate dilution. Required amount of the receptor and anions was taken directly into cuvette by using micropipette for spectroscopic titrations. The sample for ^{1}H NMR study was prepared by mixing both anion and receptor in an appropriate ratio. Then, the mixture was made soluble in DMSO-d_6, and spectrum was recorded on a Bruker Avance II 400 spectrometer by keeping tetramethylsilane (TMS) as an internal standard.

4.2 Synthesis of L^2

Receptor $\mathbf{L^2}$ was prepared by the Schiff base condensation reaction of 5-nitrosalicaldehyde (0.5 g, 0.0029 mol) with 2-aminothiophenol (0.37 g, 0.0029 mol) in methanolic medium (30 ml) at room temperature. The reaction mixture was refluxed for 1 h to obtain yellow-coloured precipitate which was washed with cold ethanol and ether. The solid obtained was recrystallised from ethanol to give yellow crystals. Yield: 90%; mp 181°C; IR (KBr pellete, υ_{max}, cm^{-1}): 3394.5, 3067.1, 2923.3, 2852.4, 2750.0, 1692.8, 1617.3, 1584.8, 1520.3, 1489.3, 1439.0, 1385.4, 1337.5, 1280.4, 1215.9, 1104.5, 987.9, 903.7, 748.5, 723.7, 708.4, 637.9; ^{1}H NMR (DMSO-d_6, δ, ppm): 4.40 (s, 1H) (SH), 7.02 (d, 1H), 7.25 (d, 1H), 7.47 (t, 1H), 7.57 (t,1H), 8.14 (m, 2H), 8.27 (s, 1H), 9.10 (s, 1H) (CH═N), 11.35 (s, 1H) (OH).

4.3 Computational methods

In order to investigate the anion-binding behaviours of the receptors, theoretical calculations were carried out with the Gaussian 09 W computer program (*33*). Optimisations of the receptors and anions have been carried out without symmetry constraints by applying HF/6-31G(d,p) method. The structural optimisation of the receptor was also examined in acetonitrile media by using the conductor-like polarised continuum model (*34*). The harmonic vibrational frequency calculations using the same methods as for the geometry optimisations were used to ascertain the presence of a local minimum.

Supporting data

Supplementary material is available online.

Acknowledgements

The authors thank Director, SV National Institute of Technology, Surat, for encouragement and for providing necessary research facilities. This work was made possible by a grant from the DST, New Delhi, under Fast Track Young Scientist Scheme.

References

(1) Bowman-James, K.; Bianchi, A.; García-Espana, E. *Anion Coordination Chemistry*; Wiley-VCH: New York, 2011.
(2) Bianchi, A.; Bowman-James, K.; Garcia-Espana, E. *Supramolecular Chemistry of Anions*; Wiley-VCH: New York, 1997.
(3) Sessler, J.L.; Gale, P.A.; Cho, W.-S. *Anion Receptor Chemistry*; Royal Society of Chemistry: Cambridge, 2006.
(4) Gunnlaugsson, T.; Glynn, M.; Tocci, G.M.; Kruger, P.E.; Pfeffer, F.M. *Coord. Chem. Rev.* **2006**, *250*, 3094–3117.
(5) Geddes, C.D. *Meas. Sci. Technol.* **2001**, *12*, R53–R88.
(6) Suksai, C.; Tuntulani, T. *Chem. Soc. Rev.* **2003**, *32*, 192–202.
(7) Martinez-Manez, R.; Sancenon, F. *J. Fluoresc.* **2005**, *15*, 267–285.
(8) Martinez-Manez, R.; Sancenon, F. *Chem. Rev.* **2003**, *103*, 4419–4476.
(9) Bazzicalupi, C.; Bencini, A.; Lippolis, V. *Chem. Soc. Rev.* **2010**, *39*, 3709–3728.
(10) Amendola, V.; Fabbrizzi, L.; Mosca, L. *Chem. Soc. Rev.* **2010**, *39*, 3889–3915.
(11) Li, A.-F.; Wang, J.-H.; Wang, F.; Jiang, Y.-B. *Chem. Soc. Rev.* **2010**, *39*, 3729–3745.
(12) (a) Gale, P.A. *Coord. Chem. Rev.* **2000**, *199*, 181–233; (b) Gale, P.A. *Coord. Chem. Rev.* **2001**, *213*, 79–128; (c) Gale, P.A. *Coord. Chem. Rev.* **2003**, *240*, 191–221; (d) Gale, P.A.; Quesada, R. *Coord. Chem. Rev.* **2006**, *250*, 3219-3244.
(13) Dydio, P.; Lichosyt, D.; Jurczak *J. Chem. Soc. Rev.* **2011**, *40*, 2971–2985.
(14) Sessler, J.L.; Camiolo, S.; Gale, P.A. *Coord. Chem. Rev.* **2003**, *240*, 17–55.
(15) (a) Xu, Z.; Kim, S.K.; Han, S.J.; Lee, C.; Kociok-Kohn, G.; James, T.D.; Yoon, J. *Eur. J. Org. Chem.* **2009**, *2009*, 3058–3065; (b) Xu, Z.; Singh, N.J.; Kim, S.K.; Spring, D.R.; Kim, K.S.; Yoon, J. *Chem. Eur. J.* **2011**, *17*, 1163–1170; (c) Zhou, Y.; Jung, J.Y.; Jeon, H.R.; Kim, Y.; Kim, S.-J.; Yoon, J. *Org. Lett.* **2011**, *13*, 2742–2745.
(16) Schmidtchen, F.P.; Berger, M. *Chem. Rev.* **1997**, *97*, 1609–1646.
(17) Li, J.-Q.; Wei, T.-B.; Lin, Q.; Li, P.; Zhang, Y.-M. *Spectrochim. Acta A* **2011**, *83*, 187–193.
(18) Zhang, J.; Lin, H.; Yu, M.; Cai, Z.; Lin, H. *Talanta* **2008**, *75*, 551–555.
(19) Zhang, Y.-M.; Lin, Q.; Wei, T.-B.; Wang, D.-D.; Yao, H.; Wang, Y.-L. *Sens. Actuators B Chem.* **2009**, *137*, 447–455.
(20) Qiao, Y.-H.; Lin, H.; Shao, J.; Lin, H.-K. *Spectrochim. Acta A* **2009**, *72*, 378–381.
(21) Mahapatra, A.K.; Manna, S.K.; Sahoo, P. *Talanta* **2011**, *85*, 2673–2680.
(22) Wang, Y.; Lin, H.; Shao, J.; Cai, Z.-S.; Lin, H.-K. *Talanta* **2008**, *74*, 1122–1125.
(23) Bao, X.; Yu, J.; Zhou, Y. *Sens. Actuators B Chem.* **2009**, *140*, 467–472.
(24) Li, Q.; Guo, Y.; Xu, J.; Shao, S. *Sens. Actuators B Chem.* **2011**, *158*, 427–431.
(25) Zang, L.; Wei, D.; Wang, S.; Jiang, S. *Tetrahedron* **2012**, *68*, 636–641.
(26) Liu, G.; Shao, J. *J. Fluoresc.* **2012**, *22*, 397–401.
(27) Sivakumar, R.; Reena, V.; Ananthi, N.; Babu, M.; Anandan, S.; Velmathi, S. *Spectrochim. Acta A* **2010**, *75*, 1146–1151.
(28) (a) Huang, W.; Lin, H.; Cai, Z.; Lin, H. *J. Incl. Phenom. Macrocycl. Chem.* **2011**, *69*, 63–68; (b) Su, H.; Huang, W.; Yang, Z.; Lin, H. *J. Incl. Phenom. Macrocycl. Chem.* **2012**, *72*, 221–225.
(29) Prabhu, S.; Saravanamoorthy, S.; Ashok, M.; Velmathi, S. *J. Lumin.* **2012**, *132*, 979–986.
(30) Hijji, Y.M.; Barare, B.; Kennedy, A.P.; Butcher, R. *Sens. Actuators B Chem.* **2009**, *136*, 297–302.
(31) Li, Q.; Guo, Y.; Xu, J.; Shao, S. *J. Photochem. Photobiol. B* **2011**, *103*, 140–144.
(32) Sahoo, S.K.; Bera, R.K.; Baral, M.; Kanungo, B.K. *J. Photochem. Photobiol. A* **2007**, *188*, 298–310.
(33) Frisch, M.J.; Trucks, G.W.; Schlegel, H.B.; Scuseria, G.E.; Robb, M.A.; Cheeseman, J.R.; Scalmani, G.; Barone, V.; Mennucci, B.; Petersson, G.A.; Nakatsuji, H.; Caricato, M.; Li, X.; Hratchian, H.P.; Izmaylov, A.F.; Bloino, J.; Zheng, G.; Sonnenberg, J.L.; Hada, M.; Ehara, M.; Toyota, K.; Fukuda, R.; Hasegawa, J.; Ishida, M.; Nakajima, T.; Honda, Y.; Kitao, O.; Nakai, H.; Vreven, T.; Montgomery, J.A.; Peralta, Jr, J.E.; Ogliaro, F.; Bearpark, M.; Heyd, J.J.; Brothers, E.; Kudin, K.N.; Staroverov, V.N.; Kobayashi, R.; Normand, J.; Raghavachari, K.; Rendell, A.; Burant, J.C.; Iyengar, S.S.; Tomasi, J.; Cossi, M.; Rega, N.; Millam, J.M.; Klene, M.; Knox, J.E.; Cross, J.B.; Bakken, V.; Adamo, C.; Jaramillo, J.; Gomperts, R.; Stratmann, R.E.; Yazyev, O.; Austin, A.J.; Cammi, R.; Pomelli, C.; Ochterski, J.W.; Martin, R.L.; Morokuma, K.; Zakrzewski, V.G.; Voth, G.A.; Salvador, P.; Dannenberg, J.J.; Dapprich, S.; Daniels, A.D.; Farkas, O.; Foresman, J.B.; Ortiz, J.V.; Cioslowski, J.; Fox, D.J. *Gaussian 09, Revision A.1*; Gaussian, Inc.: Wallingford, CT, 2009.
(34) Cossi, M.; Rega, N.; Scalmani, G.; Barone, V. *J. Comput. Chem.* **2003**, *24*, 669–681.